Development of a unified model for flow-material interaction applied to porous charring ablators

J. Coheur[1,2], A. Turchi[2], P. Schrooyen[3], T. Magin[2]

[1]Université de Liège, Liège, Belgium
[2]von Karman Institute for Fluid Dynamics, Brussels, Belgium
[3]Cenaero, Gosselies, Belgium

47th AIAA Thermophysics Conference, June 5–9, 2017
Denver, Colorado, USA
TP-04, Ablation II

Atmospheric reentry: an uncertain multiphysics problem

Main goal: Uncertainty quantification on simulations in order to assess the reliability of thermal protection systems during their design

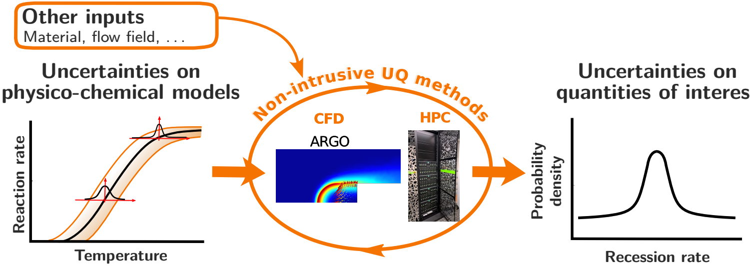

Other inputs
Material, flow field, . . .

Uncertainties on physico-chemical models

Non-intrusive UQ methods

Uncertainties on quantities of interest

Atmospheric reentry: an uncertain multiphysics problem

Main goal: Uncertainty quantification on simulations in order to assess the reliability of thermal protection systems during their design

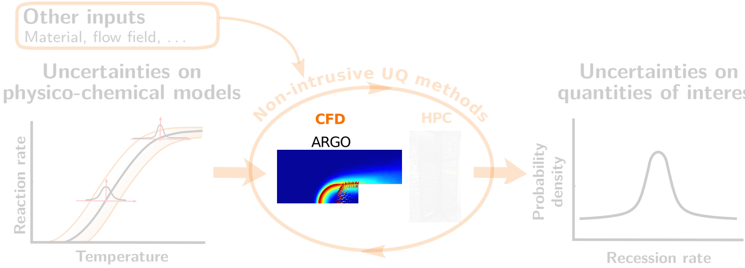

Other inputs

Material, flow field, . . .

Uncertainties on physico-chemical models

Non-intrusive UQ methods

CFD

ARGO

HPC

Uncertainties on quantities of interest

Atmospheric reentry: a complex multiphysics problem

- Need for accurate characterization of TPS for maximizing payload, ensuring safety and the success of the mission

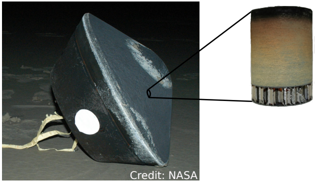
Credit: NASA

Atmospheric reentry: a complex multiphysics problem

- Need for accurate characterization of TPS for maximizing payload, ensuring safety and the success of the mission

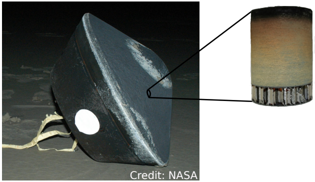
Credit: NASA

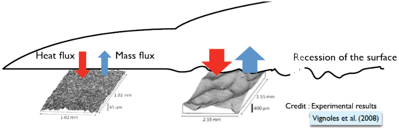

Credit : Experimental results
Vignoles et al. (2008)

- Typical mission killers
  - ➔ Non-equilibrium effects in the shock and boundary layers
  - ➔ Gas-surface interactions
  - ➔ Flow-transition from laminar to turbulent

- Our goal: develop higher fidelity tools to model those mission killers and better assist TPS design

Table of Contents

Table of Contents

Materials for TPS design

- Ablative thermal protection materials (TPMs) will allow future sample return missions and high speed re-entries!
- Investigated here: lightweight, **highly porous** ablative materials (like PICA in the US, Asterm in the EU)

Carbon preform

Credit: Mersen Scotland

Carbon/phenol composite

Credit: Airbus DS

- Carbon/phenol material = **Carbon preform** + phenolic resin

Pyrolysis-ablation problem

- When heated, the TPM is transformed and removed by two phenomena
  - pyrolysis ➔ thermal decomposition
  - ablation ➔ gas-solid reactions and transport of products, sublimation, spallation

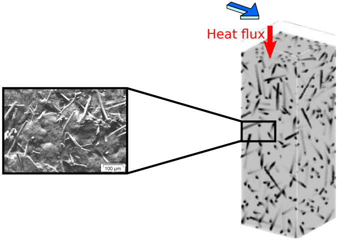

Credits: (left) Stackpoole *et al.* (2010)
(right) Lachaud *et al.* (2008)

Pyrolysis-ablation problem

- When heated, the TPM is transformed and removed by two phenomena
  - pyrolysis ➔ thermal decomposition
  - ablation ➔ gas-solid reactions and transport of products, sublimation, spallation

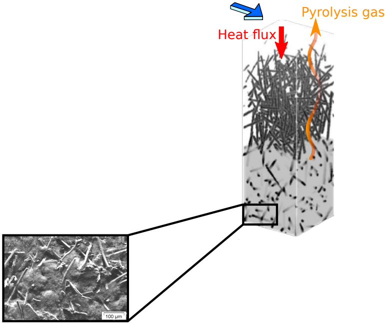

Credits: (left) Stackpoole *et al.* (2010)
(right) Lachaud *et al.* (2008)

4\. Partially ablated
3\. Charred
2\. Partially pyrolyzed
1\. Virgin material

Pyrolysis-ablation problem

- When heated, the TPM is transformed and removed by two phenomena
  - pyrolysis ➔ thermal decomposition
  - ablation ➔ gas-solid reactions and transport of products, sublimation, spallation

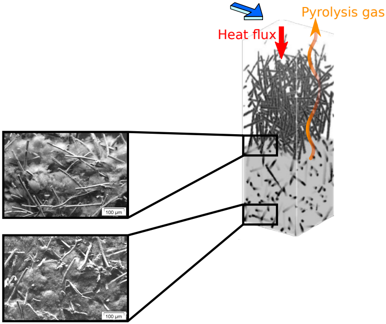

Credits: (left) Stackpoole *et al.* (2010)
(right) Lachaud *et al.* (2008)

4. Partially ablated
3. Charred
2. Partially pyrolyzed
1. Virgin material

Pyrolysis-ablation problem

- When heated, the TPM is transformed and removed by two phenomena
  - pyrolysis ➔ thermal decomposition
  - ablation ➔ gas-solid reactions and transport of products, sublimation, spallation

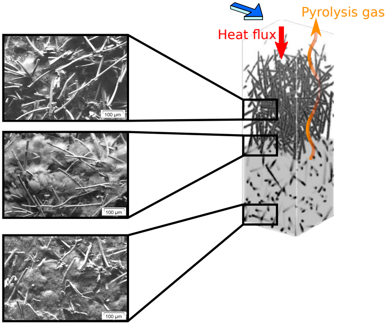

Credits: (left) Stackpoole *et al.* (2010)
(right) Lachaud *et al.* (2008)

4. Partially ablated
3. Charred
2. Partially pyrolyzed
1. Virgin material

Pyrolysis-ablation problem

- When heated, the TPM is transformed and removed by two phenomena
  - pyrolysis ➔ thermal decomposition
  - ablation ➔ gas-solid reactions and transport of products, sublimation, spallation

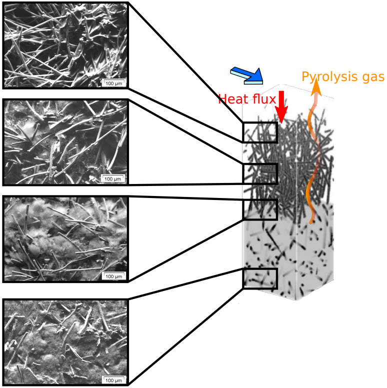

Credits: (left) Stackpoole *et al.* (2010)
(right) Lachaud *et al.* (2008)

4. Partially ablated
3. Charred
2. Partially pyrolyzed
1. Virgin material

Pyrolysis-ablation problem

- When heated, the TPM is transformed and removed by two phenomena
    - pyrolysis ➔ thermal decomposition: today
    - ablation ➔ gas-solid reactions and transport of products: yesterday (TP-02, Ablation I)

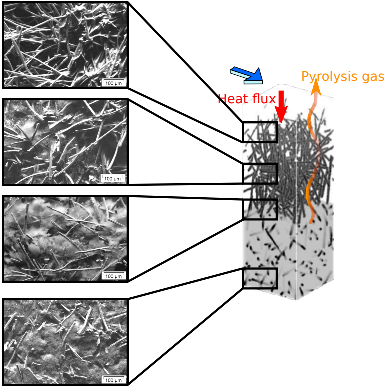

4. Partially ablated
3. Charred
2. Partially pyrolyzed
1. Virgin material

Credits: (left) Stackpoole *et al.* (2010)
(right) Lachaud *et al.* (2008)

Strategies for studying gas-surface interaction

Ground test facilities

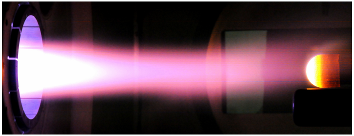

VKI Plasmatron test on carbon-phenolic
B. Helber, 2016

Numerical simulations

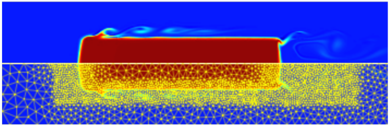

Unified flow-material approach
P. Schrooyen, 2015

Strategies for studying gas-surface interaction

Ground test facilities

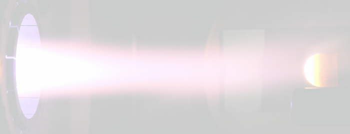

VKI Plasmatron test on carbon-phenolic
B. Helber, 2016

Numerical simulations

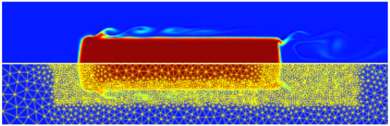

Unified flow-material approach
P. Schrooyen, 2015

Numerical approaches for studying ablation

① CFD code with ablative boundary conditions

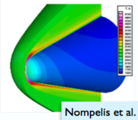

Nompelis et al. (2009)

② Material response code with heat transfer coefficients

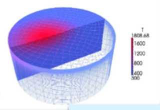

Lachaud et al. (2008)

③ Loosely coupled approach

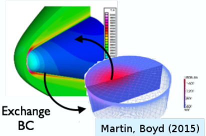

Martin, Boyd (2015)

④ **Unified approach**

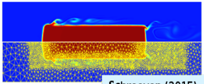

Schrooyen (2015)

Strategies for studying gas-surface interaction

Ground test facilities

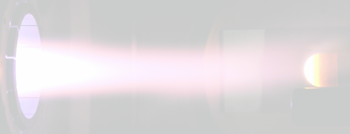

VKI Plasmatron test on carbon-phenolic
B. Helber, 2016

Numerical simulations

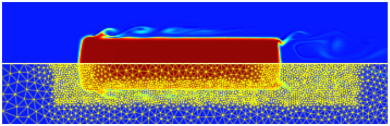

Unified flow-material approach
P. Schrooyen, 2015

Numerical approaches for studying ablation

① CFD code with ablative boundary conditions

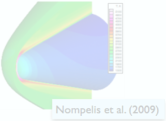

Nompelis et al. (2009)

② Material response code with heat transfer coefficients

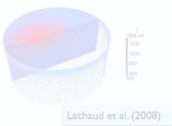

Lachaud et al. (2008)

③ Loosely coupled approach

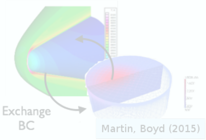

Martin, Boyd (2015)

④ **Unified approach**

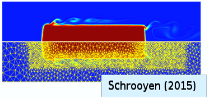

Schrooyen (2015)

Table of Contents

How to treat multiphase flows?

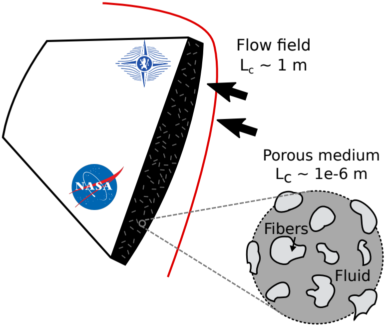

- Navier-Stokes equations for multicomponent flows valid everywhere in the fluid phase
- Chemical reactions with the solid phase

➔ Resolution too costly!

➔ Coupling the solid phase(s) with CFD not easy!

- Perform local volume averaging for a “more homogeneous” description (mesoscopic scale)
- New set of PDEs valid everywhere in the domain: Volume-Averaged Navier-Stokes (VANS) equations and chemical reaction laws

VANS equations for non-pyrolyzing media

Mass

$$\partial_t \left(\varepsilon_{\mathrm{g}} \langle \rho_i \rangle_{\mathrm{g}}\right) + \mathsf{div}_{\mathbf{x}} \left(\varepsilon_{\mathrm{g}} \langle \rho_i \rangle_{\mathrm{g}} \langle \boldsymbol{u} \rangle_{\mathrm{g}}\right) = -\mathsf{div}_{\mathbf{x}} \langle \boldsymbol{J}_i \rangle + \langle \dot{\omega}_i{}^{\mathrm{hom}} \rangle + \langle \dot{\omega}_i{}^{\mathrm{het}} \rangle \qquad (1)$$

$$\partial_t \langle \rho_{\mathrm{s}} \rangle = -\langle \dot{\omega}^{\mathrm{het}} \rangle \qquad (2)$$

Momentum

$$\partial_t (\varepsilon_{\mathrm{g}} \langle \rho \boldsymbol{u} \rangle_{\mathrm{g}}) + \mathsf{div}_{\mathbf{x}} (\varepsilon_{\mathrm{g}} \langle \rho \rangle_{\mathrm{g}} \langle \boldsymbol{u} \rangle_{\mathrm{g}} \langle \boldsymbol{u} \rangle_{\mathrm{g}}) = -\varepsilon_{\mathrm{g}} \nabla \langle p \rangle_{\mathrm{g}} + \mathsf{div}_{\mathbf{x}} \langle \boldsymbol{\tau} \rangle + \boldsymbol{F}_{\mathbf{gs}} \qquad (3)$$

Energy

$$\partial_t \langle \rho E_{\mathrm{tot}} \rangle + \mathsf{div}_{\mathbf{x}} (\varepsilon_{\mathrm{g}} \langle \rho \rangle_{\mathrm{g}} \langle H \rangle_{\mathrm{g}} \langle \boldsymbol{u} \rangle_{\mathrm{g}}) = \mathsf{div}_{\mathbf{x}} (k_{\mathrm{eff}} \nabla \langle T \rangle) + \mathsf{div}_{\mathbf{x}} (\langle \boldsymbol{\tau} \cdot \boldsymbol{u} \rangle) \qquad (4)$$

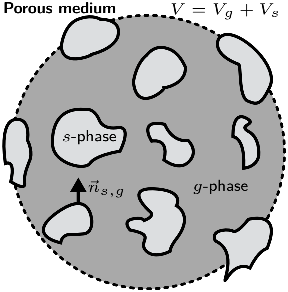

- Volume fractions

$$\varepsilon_{\mathrm{g}} = \frac{V_{\mathrm{g}}}{V}, \quad \varepsilon_{\mathrm{s}} = 1 - \varepsilon_{\mathrm{g}}$$

- Intrinsic average operator

$$\langle \alpha \rangle_\gamma = \frac{1}{V_\gamma} \int_{V_\gamma} \alpha \, dV$$

Heterogeneous chemical reactions

$$\langle \dot{\omega}_i^{\mathrm{het}} \rangle = \frac{1}{dV} \oint_{\partial\Omega_g} \underbrace{k_f^{i,C(s)} \langle \rho_i \rangle_{\mathrm{gs}}}_{\text{constant along fiber surface}} dS$$

$$= k_f^{i,C(s)} \langle \rho_i \rangle_{\mathrm{gs}} \underbrace{\frac{1}{dV} \oint_{\partial\Omega_g} dS}_{=A_{\mathrm{w}}/dV \equiv S_f}$$

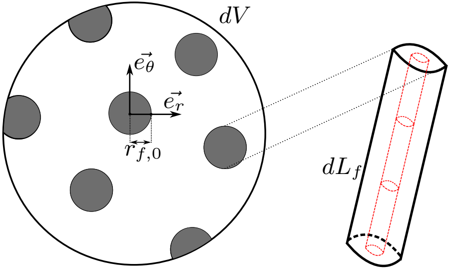

Cylindrical recession

$$S_f = \frac{2}{r_{f,0}} \sqrt{\varepsilon_{s,0} \varepsilon_s}$$

Non-constant fiber reactivity

$$S_f = \gamma \frac{A_w}{dV}$$

(see Schrooyen et al., 2016)

Implementation of a model for pyrolysis

- Mass conservation equation for a species i in gaseous phase

$$\partial_t \left(\epsilon_g \langle \rho_i \rangle_g\right) + \mathsf{div}_{\mathbf{x}}(\epsilon_g \langle \rho_i \rangle_g \langle \boldsymbol{u} \rangle_g) = -\mathsf{div}_{\mathbf{x}} \langle \boldsymbol{J}_i \rangle + \langle \dot{\omega}_i \rangle_g + \Pi_i$$

Challenges

- Modeling the decomposition of solid phases: thermal degradation, char material, protection of the fibers until resin is depleted, ...
- Treatment of several solid phases
- Characterization of the evolution of the composite porous medium
  - Thermo. and transport properties
  - Tortuosity, permeability, ...

Model for the pyrolysis decomposition

- During pyrolysis, resin matrix converts into carbon (~ 60 %), releasing gaseous products (~ 40 %)

$$\rho_m^v \rightarrow \rho_g + \rho_c$$

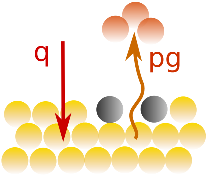

- Goldstein (1969): pyrolysis of the phenolic takes place in two main reactions

$$\frac{\partial \langle \rho_I \rangle}{\partial t} = -A_{0,I} \langle \rho_I^{\mathrm{v}} \rangle \left(\frac{\langle \rho_I \rangle - \langle \rho_I^{\mathrm{c}} \rangle}{\langle \rho_I^{\mathrm{v}} \rangle} \right)^{n_I} \exp \left(\frac{-E_I}{RT} \right), \quad I = A, B$$

- Trick, Saliba, Sandhu (1995, 1997): 4 decomposition reactions in the process!
- Local and global pyrolysis reaction advancement coefficient

$$\xi_I = \frac{\langle \rho_I^{\mathrm{v}} \rangle - \langle \rho_I \rangle}{\langle \rho_I^{\mathrm{v}} \rangle - \langle \rho_I^{\mathrm{c}} \rangle}, \quad \xi = \sum_I F_I^{\mathrm{v}} \xi_I$$

Model decomposition for charred material

- Models for charring material (Lachaud et al., 2010)

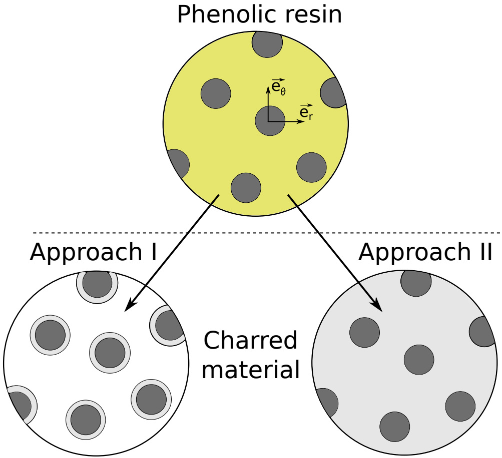

Phenolic resin

Approach I

Approach II

Charred material

Credit: Lawson *et al.*, 2010

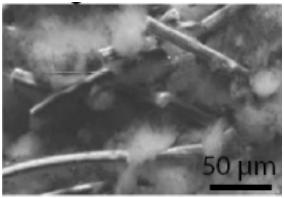

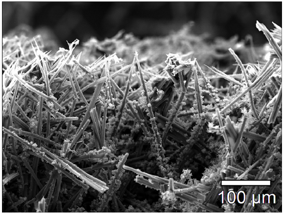

Credit: Helber *et al.*, 2015

- Matrix surrounding the fibers
- Pore-filling matrix

Matrix surrounding the fibers

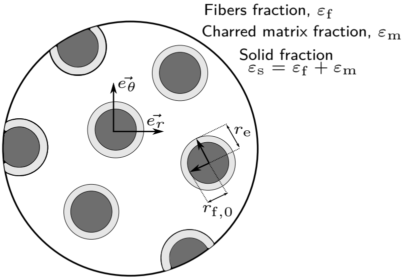

- Equivalent fibers radius

$$r_{\mathrm{e}} = r_{\mathrm{f},0} + e_{\mathrm{c}}$$

$$r_{\mathrm{e}} = r_{\mathrm{f},0}\sqrt{\frac{\varepsilon_{\mathrm{s}}}{\varepsilon_{\mathrm{f},0}}}$$

- Specific surface

$$S_{\mathrm{f}} = \frac{2}{r_{\mathrm{f},0}}\sqrt{\varepsilon_{\mathrm{f},0}\varepsilon_{\mathrm{s}}}$$

$$\frac{\partial}{\partial t}\left(\varepsilon_{\mathrm{s}}\langle\rho_{\mathrm{s}}\rangle_{\mathrm{s}}\right) = \dot{\omega}_{\mathrm{het}}$$

$$\Leftrightarrow \frac{\partial}{\partial t}\left(\varepsilon_{\mathrm{f}}\langle\rho_{\mathrm{f}}\rangle_{\mathrm{f}} + \varepsilon_{\mathrm{m}}\langle\rho_{\mathrm{m}}\rangle_{\mathrm{m}}\right) = \dot{\omega}_{\mathrm{het}}$$

$$\dot{\omega}_{\mathrm{het}} = -S_{\mathrm{f}}k_{\mathrm{f}}\langle\rho_i\rangle_{\mathrm{g}}$$

Table of Contents

Numerical modeling

- DGAblation module of Argo
- Space discretization: Discontinuous Galerkin Method (DGM)

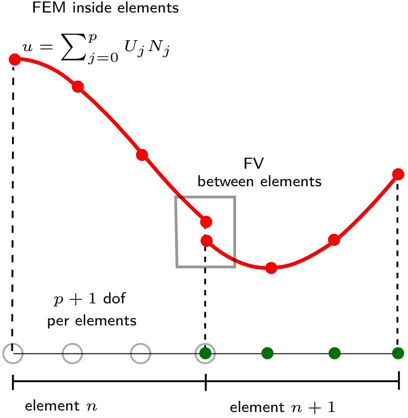

- Local conservation of physical quantities
- High order of accuracy
- Low numerical dissipation and dispersion
- Fully implicit

Hillewaert (2013), Schrooyen (2015).

Weak formulation of the convection-diffusion-reaction problem

$$\forall v \in \mathcal{V}, \quad \forall m \in N_v, \quad \int_\Omega v\mathcal{L}_m(u)d\Omega = 0 = \underbrace{\sum_{\Omega_e\in\Omega}\int_{\Omega_e} v\frac{\partial u_m}{\partial t}d\Omega_e}_{T_v}$$

$$-\underbrace{\sum_{\Omega_e\in\Omega}\int_{\Omega_e}\frac{\partial v}{\partial x^k}F_m^{c,k}(\boldsymbol{u})d\Omega_e}_{C_v} + \underbrace{\sum_{I_i\in I}\oint_{I_i}[v]^k\, n^k\mathcal{H}_m(\boldsymbol{u}^+,\boldsymbol{u}^-,\boldsymbol{n})dS}_{C_i}$$

$$+\underbrace{\sum_{\Omega_e\in\Omega}\int_{\Omega_e}\frac{\partial v}{x^k}(F_m^{d,k}(\boldsymbol{u}))d\Omega_e}_{D_v} - \underbrace{\sum_{I_i\in I}\oint_{I_i}\langle D_{mn}^{kl}\frac{\partial \boldsymbol{u}_{\boldsymbol{n}}}{\partial x^l}\rangle\,[v]^k\,dS}_{D_i}$$

$$\underbrace{-\theta\sum_{I_i\in I}\oint_{I_i}\langle D_{mn}^{kl}\frac{\partial v}{\partial x^l}\rangle\,[u_m]^k\,dS}_{D_t} + \underbrace{\alpha\sum_{I_i\in I}\oint_{I_i}[v]^k\,[u_m]^k\,dS}_{D_p}$$

$$-\underbrace{\sum_{\Omega_e\in\Omega}\int_{\Omega_e}vS(\boldsymbol{u},\nabla\boldsymbol{u})d\Omega_e}_{S_v}$$

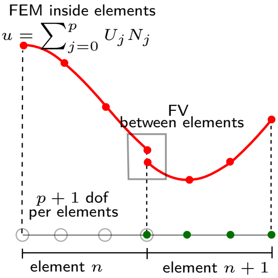

Schrooyen et al. (2016)

Table of Contents

Verification test case

- Pure conduction on a composite material

Nb of time step	Nb of elemts	Nb of DOF	Nb of CPUs	CPU time
60000	160	$160 \times 3 \times 7$ $(= 3360)$	1	≈ 5 hours

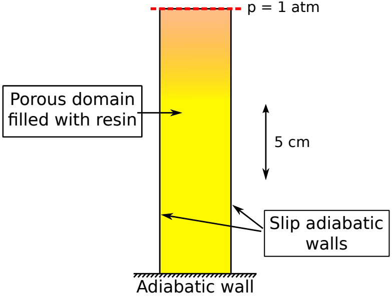

Verification test case

- Pure conduction on a composite material

Nb of time step	Nb of elemts	Nb of DOF	Nb of CPUs	CPU time
60000	160	$160 \times 3 \times 7$ $(= 3360)$	1	$\approx$ 5 hours

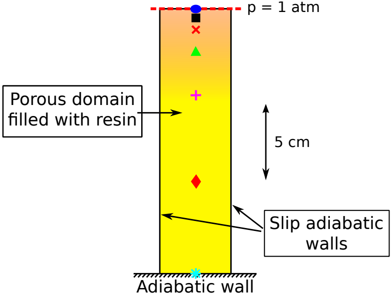

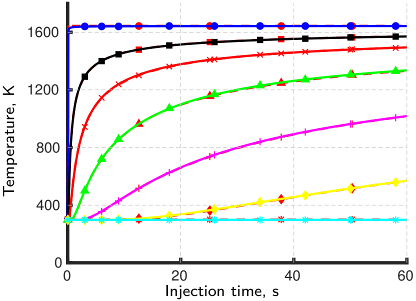

- Code-to-code verification against state-of-the art Echion solver for simple test case, using material properties of TACOT

Verification test case

- Pyrolysis of the material

Nb of time step	Nb of elemts	Nb of DOF	Nb of CPUs	CPU time
60000	160	$160 \times 3 \times 7$ $(= 3360)$	1	$\approx$ 5 hours

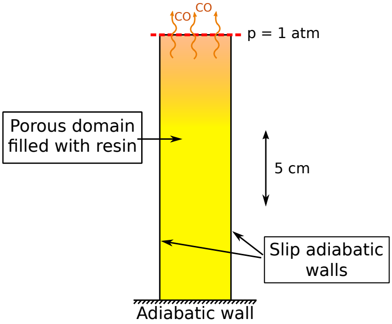

Verification test case

- Pyrolysis of the material

Nb of time step	Nb of elemts	Nb of DOF	Nb of CPUs	CPU time
60000	160	$160 \times 3 \times 7$ $(= 3360)$	1	$\approx$ 5 hours

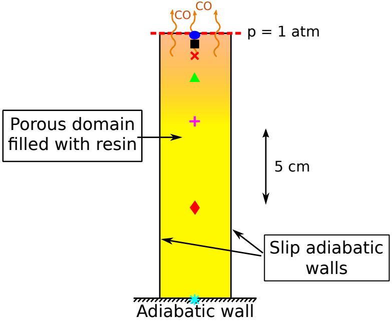

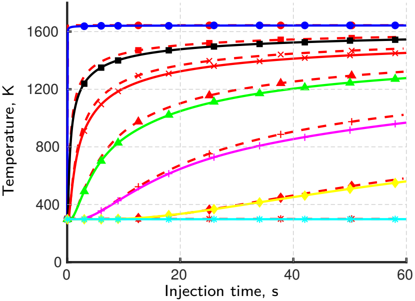

- Code-to-code verification against state-of-the art Echion solver for simple test case, using material properties of TACOT

Verification test case

- Pyrolysis of the material (cont'd)
- Comparison of pyrolysis gas blowing, char and virgin recession

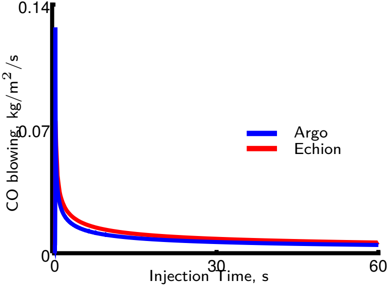

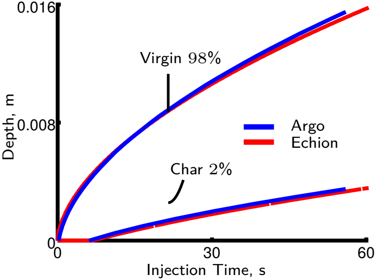

- Discrepancies accorded to the difference in momentum equations implemented inside Argo and Echion

VKI 1.2 MW Plasmatron wind tunnel

- Most powerful inductively-coupled plasma facility in the world

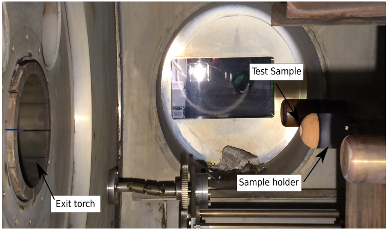

Test chamber

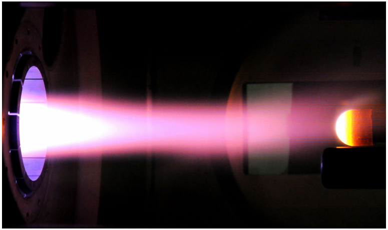

Test on a carbon-phenolic

- Test case under consideration: carbon preform sample

Test name	gas	p_s hPa	$\dot{q}_\mathrm{cw}$ kW/m^2	τ s	T_w K	$\dot{s}$ μm/s	$\dot{m}$ mg/s
HS-A2a	air	200	1016	90.4	1845	36 ± 3	60.4

B. Helber. “Material Response Characterization of Low-Density Ablators in Atmospheric Entry Plasmas”, Vrije Universiteit Brussel & von Karman Institute, 2015 (PhD Thesis).

Definition of material properties and BC

- **Plasmatron 200 hPa, 1 MW/m^2 experiment**

Material properties

- Asterm (carbon-phenolic)
- Hemispherical shape ($R = 25$ mm)
- Porosity $= 0.8$
- Permeability $= 1.2\text{e-}11$
- Tortuosity $= 1.2$
- Emissivity $= 0.97$

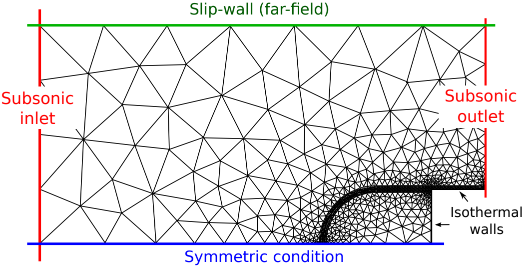

Boundary conditions

- Inlet: $U_{\text{in}} = 37$ m s^{-1}, $T_{\text{in}} = 6088$, Air$_5$ (O, O$_2$, N, N$_2$, NO) at T_{in}
- Outlet: $p_{\text{out}} = 200$ hPa
- $T_{\text{w}} = 298$ K

Material properties for unified flow approach

- No thermodynamics properties for the pure solid phase are available in open literature

➔ Adaptation of the usual TACOT properties using `Mutation++` with air

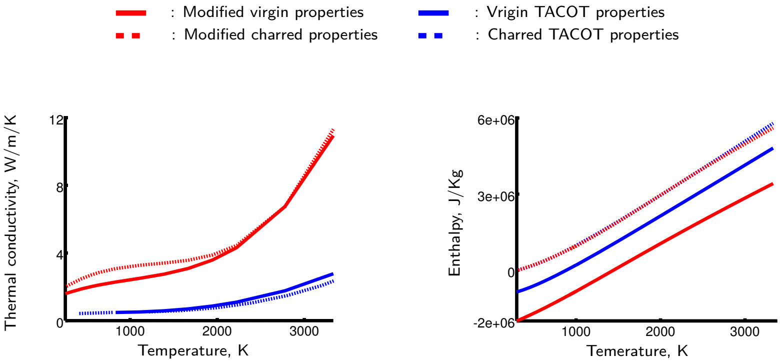

Results: flow fields after $t = 0.4$ s

Nb of time steps	Nb of elemts	Nb of DOFs	Nb of CPUs	CPU time
81198	2250	$2250 \times 3 \times 12$ $(= 81000)$	12	$\approx$ 2 weeks

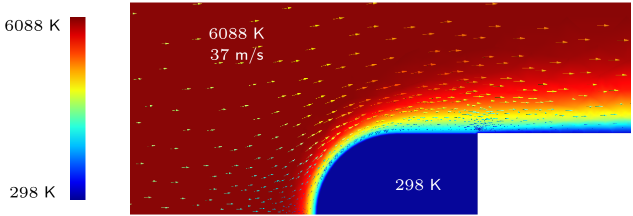

Temperature and vector flow field

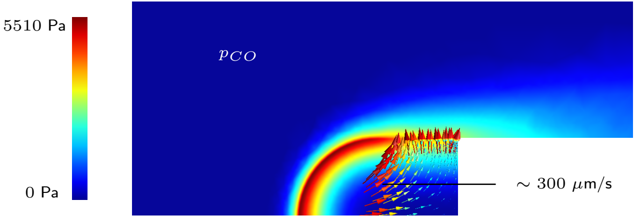

CO pressure field

Results: total pressure and mass fractions

- Total pressure along stagnation line

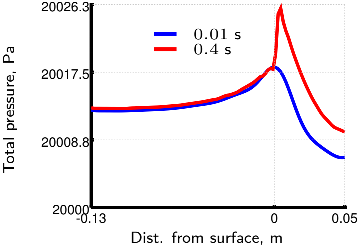

- Mass fractions along stagnation line

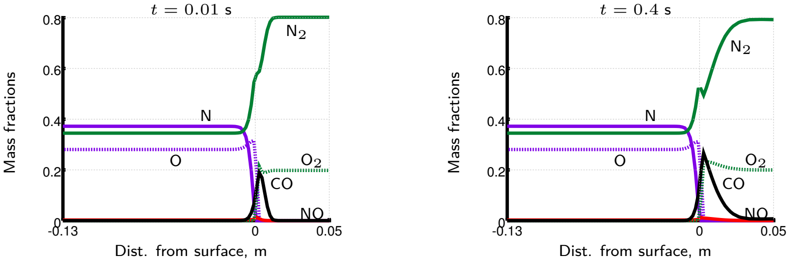

Results: total pressure and mass fractions

- Total pressure along stagnation line

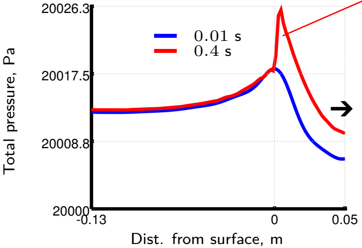

Max. peak shift

O_2 not consumed inside the material!

➔ Sharp increase of pressure!

- Mass fractions along stagnation line

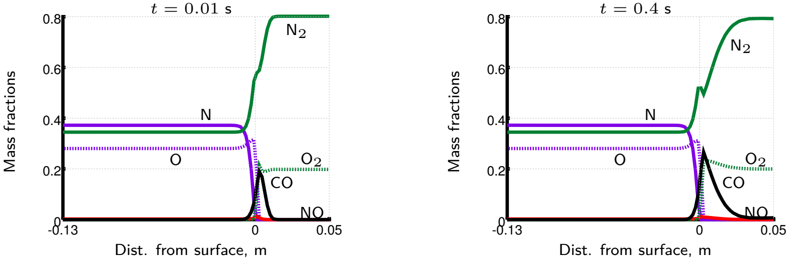

Table of Contents

Conclusion and outlook

Implementation of a new module for pyrolysis using the unified approach:

- One mass conservation equation per resin compounds
- Pure conduction/pyrolysis decomposition model verified on state-of-the-art test cases
- Model for charred material surrounding the fibers implemented
- Preliminary simulations of Plasmatron experiments on pyrolyzing materials

➔ **One of the first unified flow-material solver featuring pyrolysis**

Conclusion and outlook

Implementation of a new module for pyrolysis using the unified approach:

- One mass conservation equation per resin compounds
- Pure conduction/pyrolysis decomposition model verified on state-of-the-art test cases
- Model for charred material surrounding the fibers implemented
- Preliminary simulations of Plasmatron experiments on pyrolyzing materials

➔ One of the first unified flow-material solver featuring pyrolysis

Outlook:

- Verification and validation of the charred model
- Simulations with real material properties/pyrolysis gas composition
- Comparison with Plasmatron experiments on carbon phenol materials

Development of a unified model for flow-material interaction applied to porous charring ablators

J. Coheur[1,2], A. Turchi[2], P. Schrooyen[3], T. Magin[2]

[1]Université de Liège, Liège, Belgium
[2]von Karman Institute for Fluid Dynamics, Brussels, Belgium
[3]Cenaero, Gosselies, Belgium

47th AIAA Thermophysics Conference, June 5–9, 2017
Denver, Colorado, USA
TP-04, Ablation II

Bibliography

- G. Duffa. *Ablative Thermal Protection Systems Modeling*. American Institute of Aeronautics and Astronautics, Inc., Reston, Virginia, 2013.
- J. Lachaud, I. Cozmuta, N. N. Mansour. *Multiscale Approach to Ablation Modeling of Phenolic Impregnated Carbon Ablators*. Journal of Spacecraft and Rockets, Vol. 47, No. 6 (2010), pp. 910-921.
- J. Lachaud, T.E. Magin, I. Cozmuta and N.N. Mansour. *A Short Review of Ablative-Materials Response Models and Simulation Tools*. 7th European Symposium on Aerothermodynamics, Brugge, Belgium, 2011.
- P. Schrooyen. *Numercial Simulation of Aerothermal Flows Through Ablative Thermal Protection Systems*. PhD Thesis. UCL & VKI, 2015.
- B. Helber. *Material Response Characterization of Low-Density Ablators in Atmospheric Entry Plasmas*. PhD Thesis. ULB & VKI, 2015.